Three-Dimensional Nuclear Analysis for the US Dual Coolant Lithium Lead ITER Test Blanket Module

M.E. Sawan, B. Smith, E.P. Marriott, P.P.H. Wilson

December 2010

UWFDM-1380

Published in *Fusion Engineering and Design*, 85 (2010) 1027-1032.

FUSION TECHNOLOGY INSTITUTE

UNIVERSITY OF WISCONSIN

MADISON WISCONSIN

Three-Dimensional Nuclear Analysis for the US Dual Coolant Lithium Lead ITER Test Blanket Module

M.E. Sawan, B. Smith, E.P. Marriott, P.P.H. Wilson

Fusion Technology Institute
University of Wisconsin
1500 Engineering Drive
Madison, WI 53706

http://fti.neep.wisc.edu

December 2010

UWFDM-1380

Published in *Fusion Engineering and Design*, 85 (2010) 1027-1032.

Abstract

Detailed 3-D neutronics calculations have been performed for the US DCLL TBM. The neutronics calculations were performed directly in the CAD model using the DAG-MCNP code that allows preserving the geometrical details. Detailed high-resolution, high-fidelity profiles of the nuclear parameters were generated using fine mesh tallies. These included tritium production, nuclear heating, and radiation damage. The TBM heterogeneity, exact source profile, and inclusion of the surrounding frame and other in-vessel components result in lower TBM nuclear parameters compared to the previous 1-D predictions. This work clearly demonstrates the importance of preserving geometrical details in nuclear analyses of geometrically complex components in fusion systems.

1. Introduction

In support of the ITER Test Blanket Module (TBM) program [1], the US has been developing a TBM design based on the dual coolant lead lithium (DCLL) blanket concept [2]. The basic idea of the DCLL blanket is to use helium to remove all heat deposited in the first wall (FW) and blanket structure, and a flowing, self-cooled, lead lithium eutectic (PbLi) breeder (with Li enriched to 90% Li-6) to remove nuclear heat generated in the breeding zone at a high temperature for efficient power conversion [2]. This is the preferred US blanket concept for commercial fusion plants.

The concept consists of PbLi channels contained within a helium-cooled structure made of reduced activation ferritic steel (RAFS). Each PbLi channel is lined with a SiC flow channel insert (FCI) that separates the PbLi from the RAFS structure. This FCI performs two important functions: (a) thermally insulates the PbLi so that its temperature can be considerably higher than the surrounding structure, and (b) provides electrical insulation between the PbLi flow and the thick, load-bearing RAFS walls to reduce the MHD pressure drop. The concept will be tested in one half of a designated test port where it will be mounted inside a water-cooled frame. Many design issues were considered in determining the configuration of the TBM. That includes both PbLi and He manifolding and flow path arrangement. The same nuclear data (FENDL-2.1) and neutron source strength were used in both 3-D and 1-D calculations.

The design has been evolving over the past several years following several technical reviews and it converged on a reference design for which detailed CAD models were generated. The overall dimensions of the TBM are 166 cm in height, 48.4 cm in width, and 35 cm in thickness. In addition, the reference TBM design utilizes a flat front surface. The PbLi flow starts at the top flowing downward in the back channel then upward in the front channel. Helium flow in the FW has two circuits with 7 passes per circuit. Grid plates are used to route the flow radially. Fig. 1 shows the overall DCLL TBM configuration with an exploded view showing the internal components. Detailed three-dimensional (3-D) neutronics calculations were performed for the reference design configuration based on the detailed CAD model. In this paper, the relevant nuclear performance parameters for the reference DCLL TBM design are presented and compared

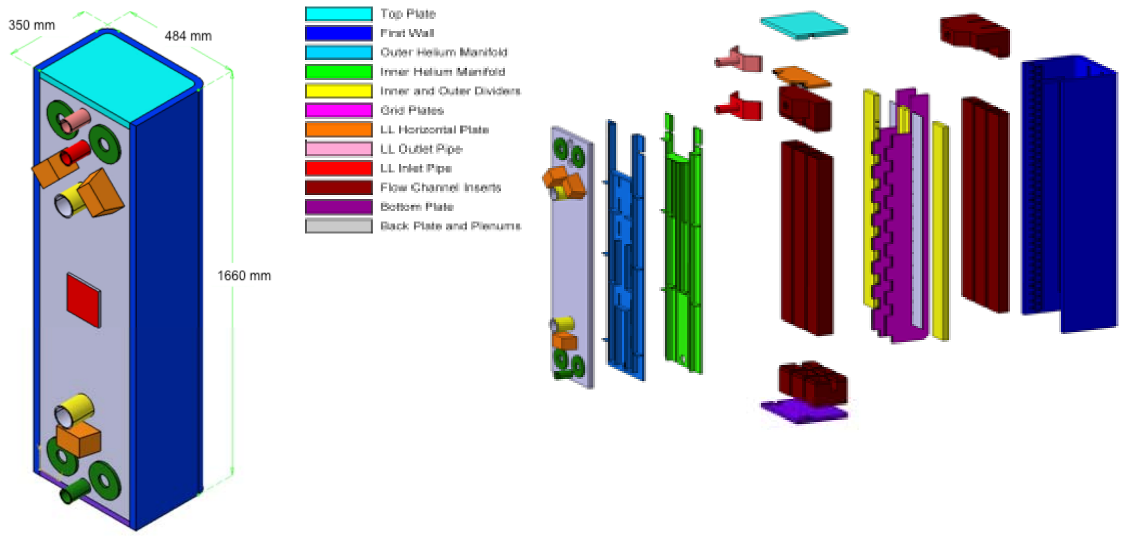

Fig. 1. DCLL TBM configuration with exploded view.

to previous estimates from 1-D calculations [3]. These include tritium breeding, nuclear heating, and radiation damage.

2. Neutronics calculation procedure

It is clear from Fig. 1 that the geometrical configuration of the TBM is quite complex and detailed 3-D calculations are required to accurately account for the geometrical details. The neutron and gamma fluxes and energy spectra in the different components of the TBM are affected by other components in the ITER plasma chamber. The 3-D model should properly account for the tokamak configuration with the accurate source profile. We performed 3-D neutronics for the DCLL TBM using the Direct Accelerated Geometry MCNP (DAG-MCNP) code [4] where the neutronics calculations are performed directly in the CAD model. This allows preserving the geometrical details without any simplification and eliminates possible human error in modeling the geometry.

The CAD model developed for the DCLL TBM was inserted in the CAD model for the frame. Since we are interested in nuclear parameters in the TBM itself, a simplified CAD model with homogenized zones was generated and used for the frame as shown in Fig. 2. The integrated

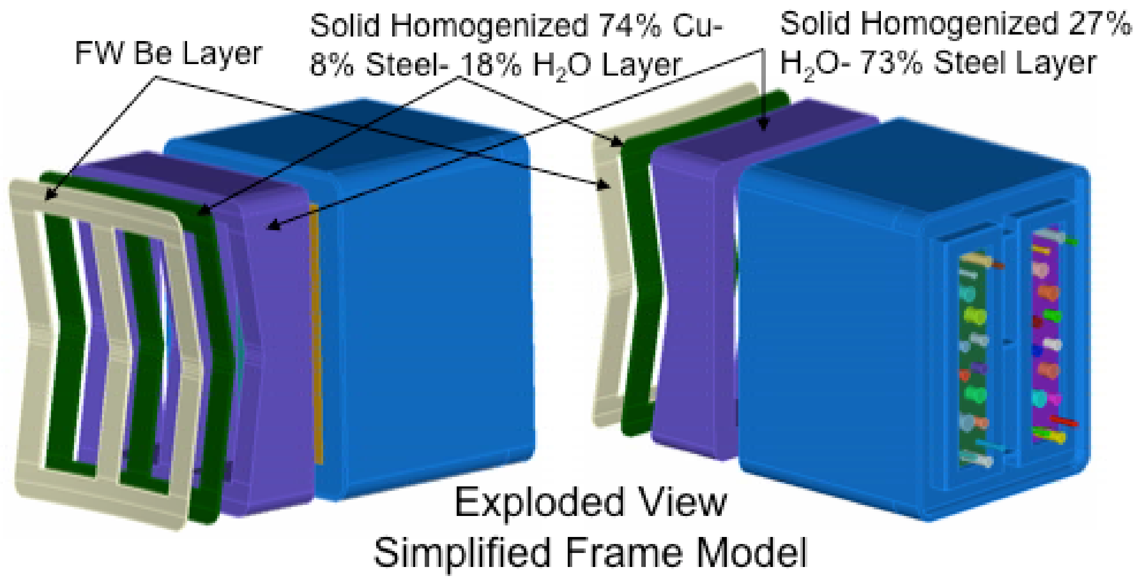

Fig. 2. Frame CAD model used in analysis.

CAD model has been “cleaned” to eliminate any geometrical clashes before using it in the analysis. The helium coolant in the TBM is represented by void in the model. A separate PbLi volume was generated in the CAD model to distinguish between He and PbLi coolant/breeder regions and allow calculating nuclear parameters in the PbLi zones.

In order to accurately represent the source profile in the plasma and account for secondary contribution from other components in the ITER plasma chamber, we utilized the surface source write/read feature in DAG-MCNP. The calculations were performed in steps. In the first step, a simplified CAD model based on a 40° sector of ITER that includes all ITER components, with detailed structures in each component being suppressed using homogenized material definitions, was used. The model includes dummy port plugs in the equatorial ports. This model was previously used in ITER neutronics benchmark calculations [5]. The neutron source was sampled from the exact ITER neutron source profile. An extra surface was inserted into the ITER geometry in front of the equatorial port. All particles crossing this surface were recorded according to their location, angle, energy, and weight. Fig. 3 shows the energy spectrum of neutrons incident on the TBM from the surface source. Only 52% of the neutrons incident on the TBM are at 14 MeV due to the significant secondary component from other chamber

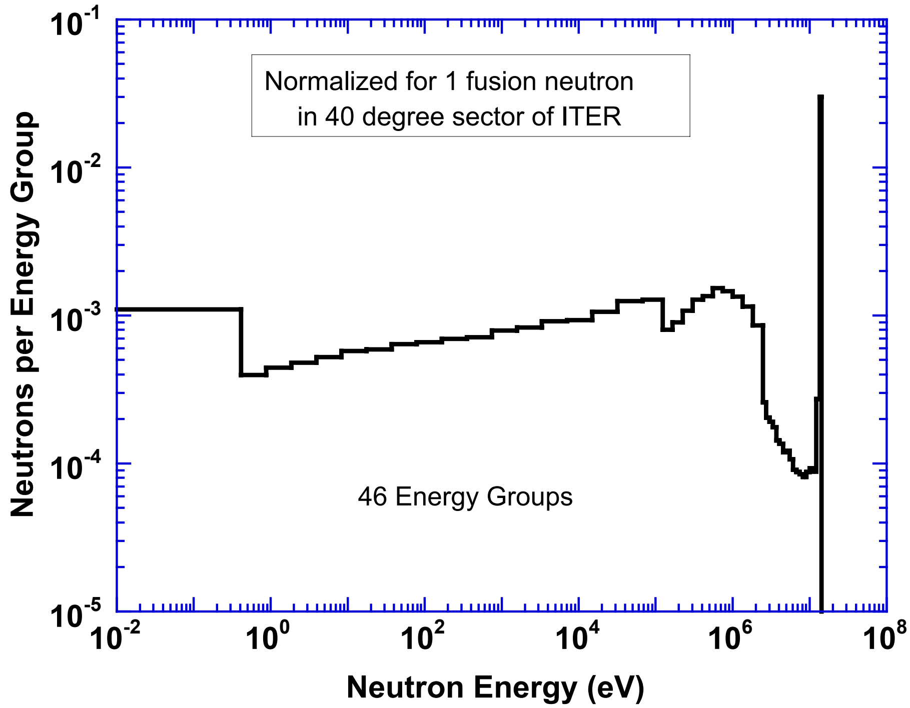

Fig. 3. Energy spectrum of neutrons incident on TBM.

components. The average neutron energy is 7.75 MeV. The number of secondary gamma photons incident on the TBM is 37% of the number of neutrons with an average energy of 1.48 MeV. The neutrons have more perpendicular angular distribution compared to the mostly tangential secondary gammas.

In the second step, these parameters are read as a surface source in front of the detailed integrated frame/TBM CAD model. While the effect of reflection into the chamber from the in-vessel components is accounted for by the surface source, contribution at the sides of the TBM will depend on the boundary conditions used in the second step of the calculation [6]. To investigate the sensitivity of TBM local parameters to addition of frame and surrounding shield modules, we performed several 2-D calculations that indicated that the 20 cm thick frame results in neutronics decoupling between the TBM and adjacent shield modules with <2% effect on local parameters. On the other hand, the frame in the model has significant effect on the DCLL TBM local parameters (up to 30%) and should be included in the model. In addition, assessment of surface source utilization indicated that it yields exact results, comparable to the full chamber

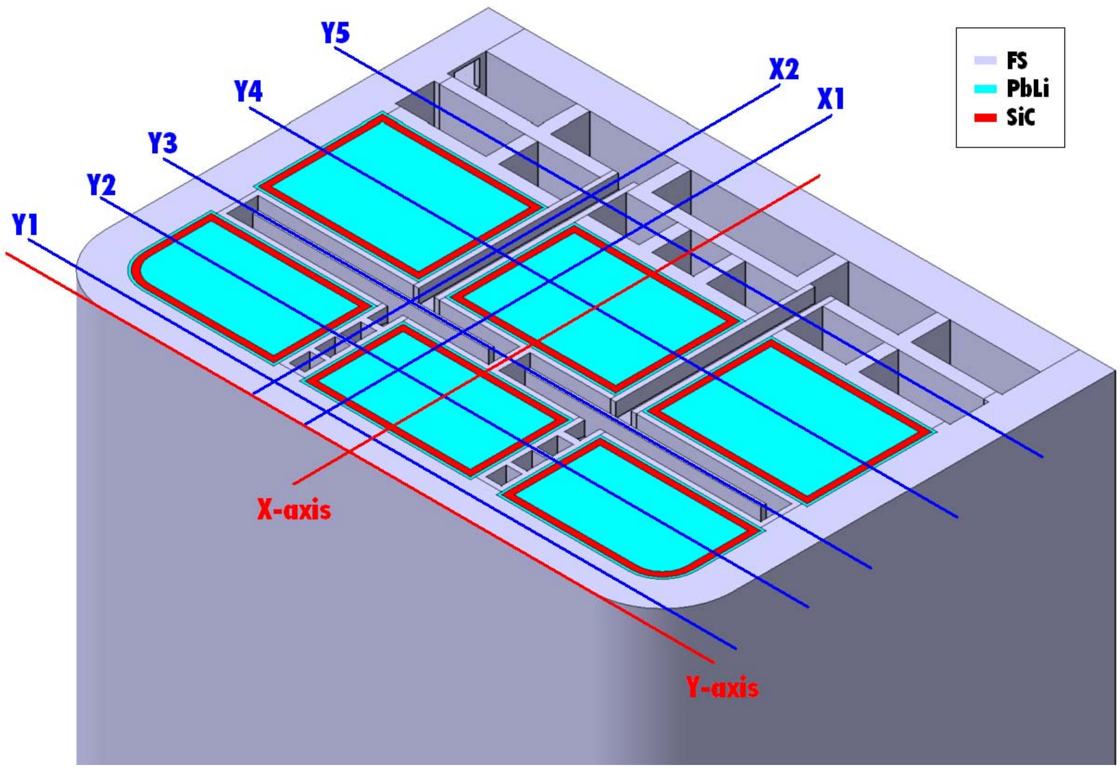

Fig. 4. Cross section at mid-plane of TBM.

analysis, if the surface source is extended at least 10 cm beyond the analyzed module [6]. Accordingly, we used the surface source with the integrated frame/TBM model surrounded with reflecting boundaries at its four sides. Only half of the frame with a DCLL TBM inserted in it was used in the analysis. Detailed maps of nuclear parameters were generated in the TBM. We used 50 million source particles in the full ITER calculation. Of those, 4.2 million surface crossings were written to the surface source file in a run that took 5.7 days. The surface source file was read 20 times with different random numbers, for a total of one billion ITER source particles in a run that took 4.55 days. 19 mesh tallies were used with different mesh sizes in the range 2 to 20 mm. Fig. 4 gives a horizontal cross section at the TBM mid-plane with sections identified at which fine mesh tallies are used for nuclear parameter mapping.

3. Tritium breeding

The spatial distribution of tritium production rate at mid-plane is given in Fig. 5 along with a detailed configuration of materials at that section. Tritium production in the front Be layer is

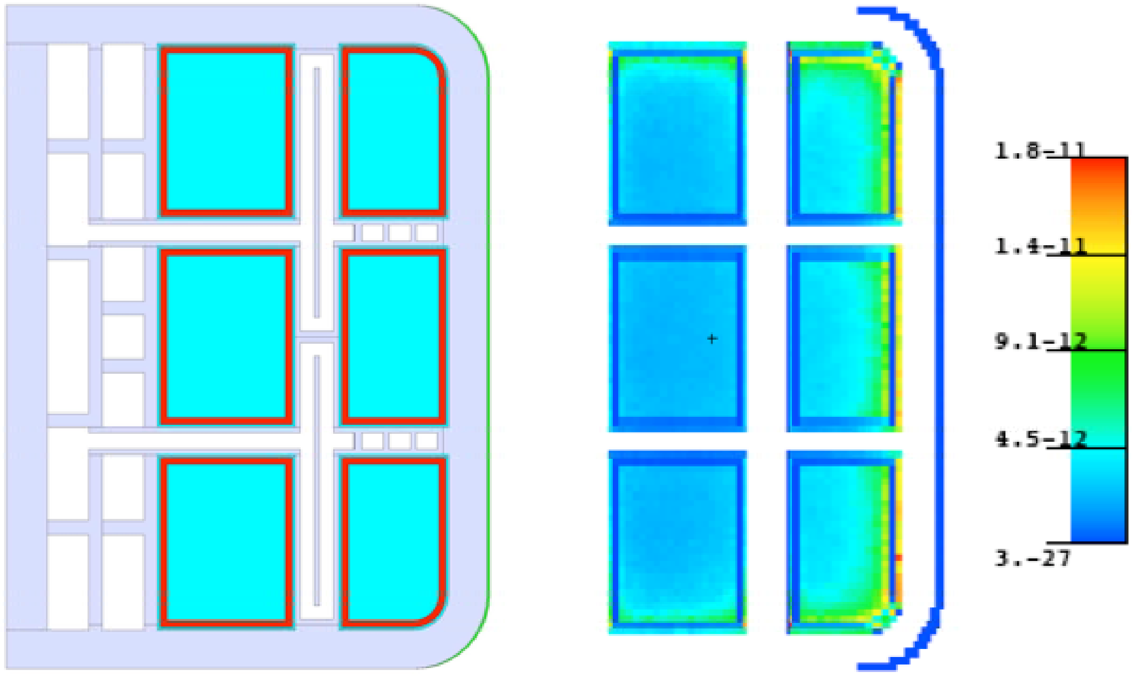

Fig. 5. Tritium production (g/cm^3s) at mid-plane of TBM.

much lower than that in the front regions of PbLi. During the 500 MW D-T pulse, the peak tritium production rate in PbLi is $2.8x10^{-11}$ g/cm^3s and that in the 2 mm plasma facing beryllium layer is only $7.7x10^{-13}$ g/cm^3s. Tritium production is higher at the edges of the module due to the softer neutron spectrum from slowing down in the water in the surrounding frame leading to higher breeding in Li-6. During the D-T pulse, tritium is produced in the PbLi at the rate of $4.19x10^{-7}$ g/s. For a pulse with 400 s flat top preceded by 20 s linear ramp-up to full power and followed by 20 s linear ramp-down, the total tritium generation in PbLi is $1.76x10^{-4}$ g/pulse. For the planned 3000 pulses per year the annual tritium production in the PbLi is 0.53 g/year. The tritium inventory in the TBM at any time will be much smaller since tritium will be continuously extracted from the PbLi. The corresponding annual tritium production in the Be is $1.04x10^{-3}$ g/year representing only 0.2% of the total tritium production in the TBM. The detailed 3-D analysis with the surrounding massive water-cooled frame and representation of the exact source and other in-vessel components yields total tritium production in the TBM that is 45% lower than the previous 1-D estimate [3]. This is attributed to the lower reflection from the in-vessel

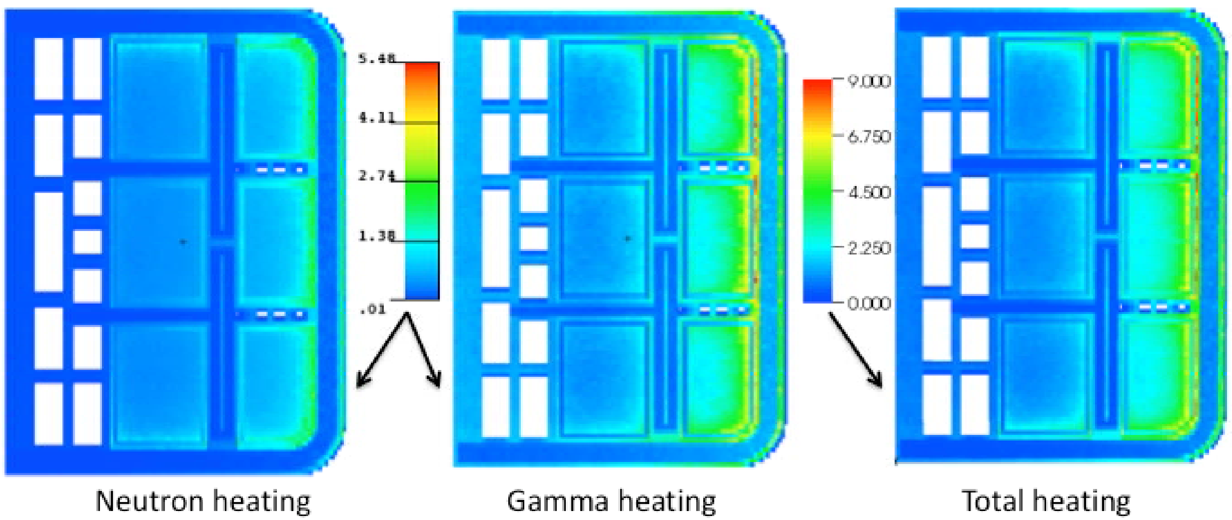

Fig. 6. Nuclear heating (W/cm^3) distribution at mid-plane section.

components and additional absorption in the surrounding frame compared to the 1-D analysis where a DCLL blanket is effectively assumed to replace other chamber components and frame.

4. Nuclear heating

The nuclear heating distribution is shown in Fig. 6 at mid-plane. Detailed maps of neutron, gamma, and total heating (W/cm^3) are provided. The impact of the material heterogeneity of the nuclear heating distribution is clearly demonstrated. Gamma heating in PbLi is higher than in adjacent SiC FCI while neutron heating in SiC is higher than that in PbLi. Be PFC has lower gamma heating than the FS in the FW but has higher neutron heating. The sides of the TBM adjacent to the water-cooled steel frame show higher gamma heating in PbLi due to gamma generation in steel and water and neutron heating is also higher due to neutron slowing down in water leading to larger neutron heating in Li-6. Figs. 7 and 8 show total nuclear heating distribution at sections Y2 and X1. The slight shift of peak from mid-plane reflects the vertical shift in peak source strength.

Table 1 compares the peak power densities in the TBM constituent materials during the 500 MW D-T pulse. Peak values obtained from the previous 1-D calculations [3] are also included for comparison. It is clear that detailed 3-D analysis of the TBM yields lower peak nuclear

Table 1. Peak nuclear heating in TBM constituent materials

Material	Neutron Heating (W/cm^3)	Gamma Heating (W/cm^3)	Total Nuclear Heating (W/cm^3)	Peak Nuclear Heating from 1-D Calculations
Ferritic Steel	1.38	4.70	6.08	9.20
Lead Lithium	4.11	5.48	9.59	13.20
SiC FCI	2.74	1.38	4.12	4.79
Be PFC	5.48	1.00	6.48	8.14

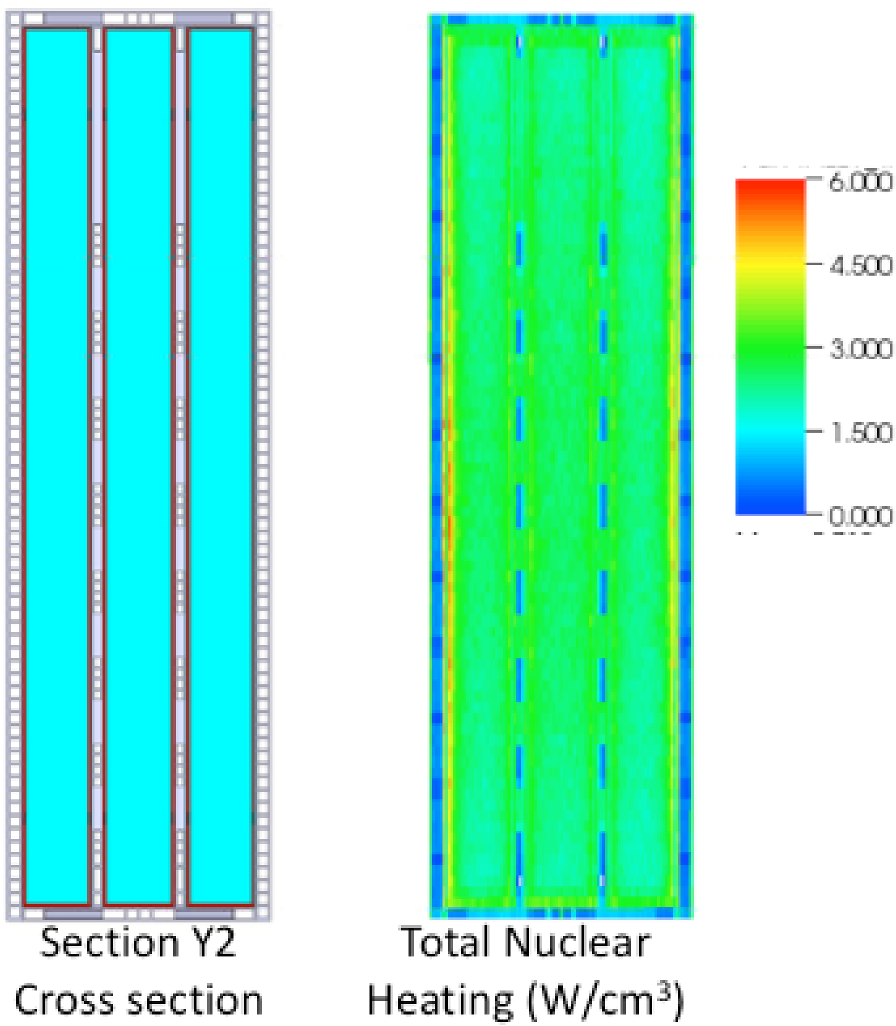

Fig. 7. Total nuclear heating at section Y2.

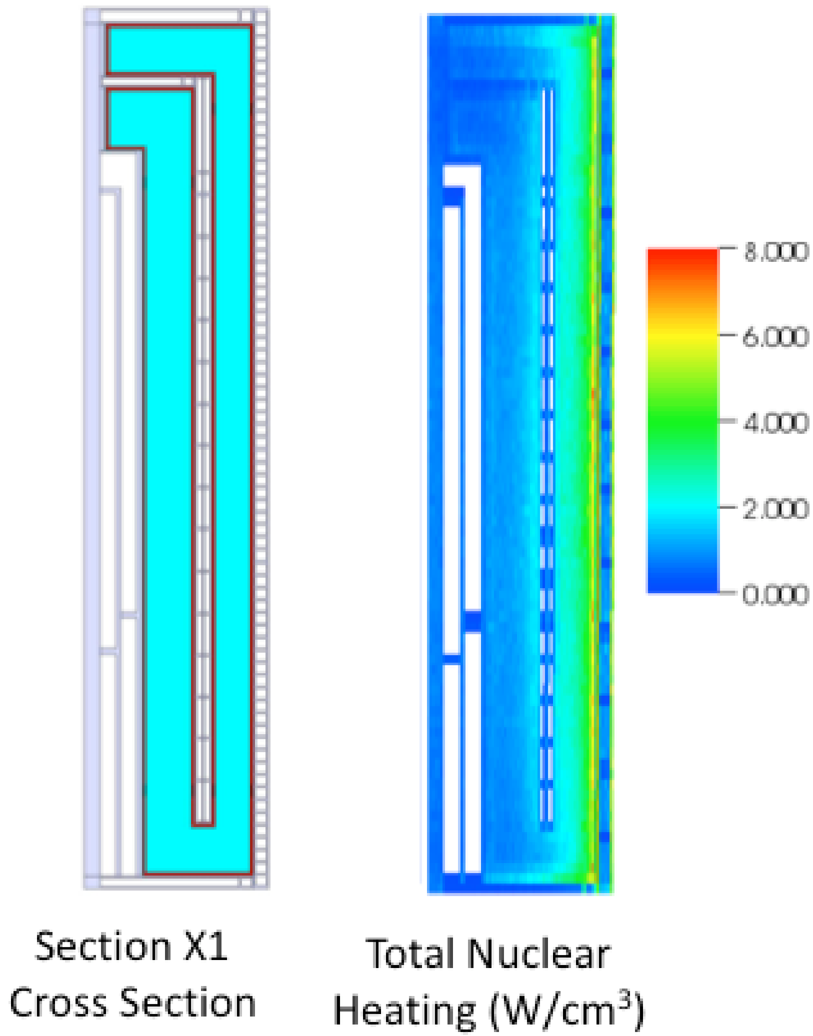

Fig. 8. Total nuclear heating at section X1.

heating values in the TBM materials compared to the 1-D estimates. Table 2 gives total nuclear heating generated in the different materials of the TBM. The total TBM thermal power is 0.614 MW which includes 0.24 MW surface heating and 0.374 MW volumetric nuclear heating. The detailed 3-D analysis of the TBM yields total nuclear heating in the TBM that is 35% lower than the 1-D estimate of 0.574 MW. The reduced total heating is due to less reflection from the in-vessel components in the 3-D model compared to full coverage with the DCLL TBM in the 1-D analysis. In addition, the surrounding water-cooled steel frame acts as a strong sink for neutrons.

Table 2. Total nuclear heating in TBM

Material	Total Nuclear Heating (MW)
Ferritic Steel	0.121
Lead Lithium	0.218
SiC FCI	0.028
Be PFC	0.007

5. Structure radiation damage

The detailed spatial distributions of ferritic steel atomic displacement damage (dpa) and helium production rates were determined in the TBM. Fig. 9 shows maps of dpa and helium production rates at sections Y1 (along FW) and X1 (across depth of TBM). These values were calculated for steel everywhere even in PbLi and He regions. The peak damage parameters in the FW occur at the center due to enhanced neutron multiplication in the PbLi. Lower damage parameters occur in the outer regions of the TBM adjacent to the frame due to neutron absorption and slowing down in the water-cooled steel frame. The peak dpa and He production rates in the ferritic steel structure are 7 dpa/FPY and 97 He appm/FPY. For the average ITER neutron wall loading of 0.57 MW/m^2 and the total fluence goal of 0.3 MWa/m^2, the total full power lifetime is 0.526 FPY. The peak cumulative end-of-life dpa in the FW is 3.7 dpa and the peak end-of-life helium production is 51 He appm. The detailed 3-D analysis of TBM with the surrounding massive water-cooled frame and representation of exact source and other in-vessel components yields 28% lower peak dpa rate and 10% lower peak He production rate in the FW compared to the 1-D estimates. This is due to the more perpendicular angular distribution of incident source neutrons in the realistic 3-D configuration and reduced neutron multiplication and reflection from surrounding frame and other in-vessel components compared to the 1-D configuration with full coverage with DCLL TBM. The effect on He production is less than that on dpa since helium is produced by higher energy neutrons.

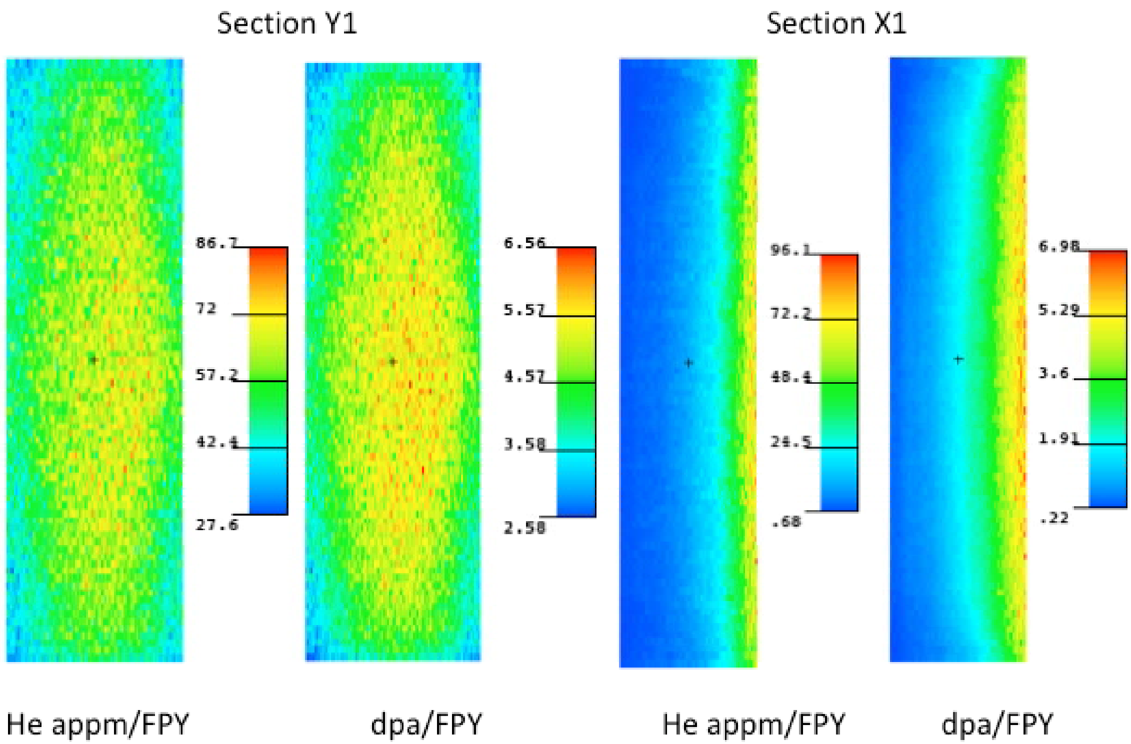

Fig. 9. Radiation damage profiles along two sections in the TBM.

6. Summary and conclusions

Detailed 3-D neutronics calculations have been performed for the US DCLL TBM to accurately account for the complex geometrical heterogeneity and impact of source profile and other in-vessel components. The neutronics calculations were performed directly in the CAD model using the DAG-MCNP code that allows preserving the geometrical details. The 20 cm thick frame results in neutronics decoupling between the TBM and adjacent shield modules. The TBM CAD model was inserted in the CAD model for the frame and the integrated CAD model was used in the 3-D analysis. Detailed high-resolution, high-fidelity profiles of the nuclear parameters were generated using fine mesh tallies. The TBM heterogeneity, exact source profile, and inclusion of the surrounding frame and other in-vessel components result in lower TBM nuclear parameters compared to the 1-D predictions. This work clearly demonstrates the importance of preserving geometrical details in nuclear analyses of geometrically complex components in fusion systems.

Acknowledgement

This work has been performed through grants from the US Department of Energy.

References

[1] M. Abdou, D. Sze, C. Wong, M. Sawan, A. Ying, N. Morley, and S. Malang, U.S. plans and strategy for ITER blanket testing, Fusion Sci. Technol., 47 (3) (2005) 475-487.

[2] C.P.C. Wong, S. Malang, M. Sawan, M. Dagher, S. Smolentsev, B. Merrill, et al., An overview of dual coolant Pb–17Li breeder first wall and blanket concept development for the US ITER-TBM design, Fusion Eng. Des., 81 (2006) 461-467.

[3] M.E. Sawan, E.P. Marriott, M. Dagher, Neutronics performance parameters for the US dual coolant lead lithium ITER test blanket module, in: Proceedings of the 23nd IEEE/NPSS Symposium on Fusion Engineering (SOFE), May 31-June 5, 2009, San Diego, CA.

[4] T. Tautges, P.P.H. Wilson, J. Kraftcheck, B. Smith, and D. Henderson, Acceleration techniques for direct use of CAD-based geometries in Monte Carlo radiation transport, in: Proceedings of International Conference on Mathematics, Computational Methods & Reactor Physics (M&C 2009), Saratoga Springs, New York, May 3-7, 2009.

[5] P.P.H. Wilson, R. Feder, U. Fischer, et al., State of the art 3-D radiation transport methods for fusion energy systems, Fusion Eng. Des., 83 (2008) 824-833.

[6] T.D. Bohm, B. Smith, M.E. Sawan, and P.P.H. Wilson, Assessment of using the surface source approach in 3-D neutronics of fusion systems, University of Wisconsin Fusion Technology Institute, UWFDM-1368 (2009).